

EVALUATION OF DENOISING ALGORITHMS APPLIED TO THE REDUCTION OF SPECKLE IN DIGITAL HOLOGRAPHY

S. Montresor^{}, P. Y. Quehe[†], S. Verhaeghe[†], P. Picart^{*†}*

^{*} Laboratoire d'Acoustique de l'Université du Maine, UMR CNRS 6613,
avenue Olivier Messiaen, 72085 Le Mans cedex 09, France.

[†] Ecole Nationale Supérieure d'Ingénieurs du Mans,
rue Aristote, 72085 Le Mans cedex 09, France.

ABSTRACT

In this article we compare image denoising algorithms applied to laser digital holography technique. The presented work focuses on reducing speckle noise contribution. The evaluation methodology lies on images of synthesized phases of which one controls the level and noise type. We retain five algorithms known for their efficiency in the field of image processing. These are: algorithms used for SAR filtering (Synthetic Aperture Radar), algorithms based on wavelets, the NLmeans algorithm recently proposed, the Wiener filter and the median filter. Three evaluation criteria are used to compare selected algorithms: the gain of SNR and quality index; we propose also a new one: the reconstructed phase error which is particularly relevant in the domain of digital holography.

Index Terms— denoising, image processing, speckle noise, phase, wavelets

1. INTRODUCTION

Digital holographic interferometry is an optical technique using coherent light. It is widely used for field displacement and surface shapes measurements. Its main advantage is that it allows characterization of rough surfaces of objects with a high precision by contactless measurement.

1.1. Digital Holography Principle

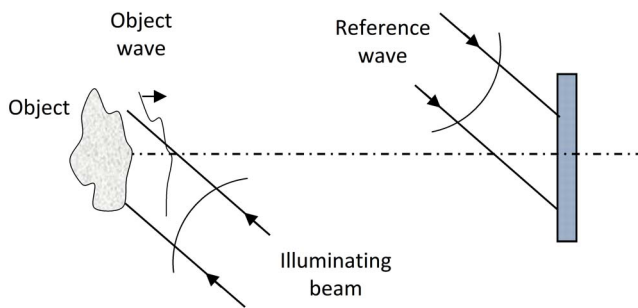
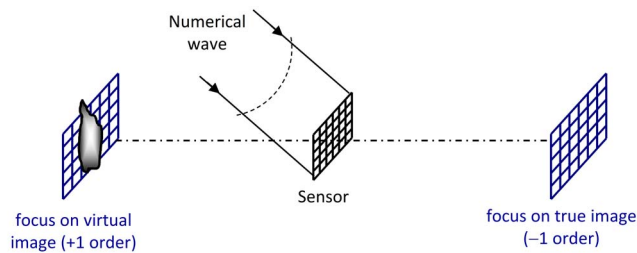
The principle of digital holography is based on the coherent mixture of a so called reference wave and a so called object wave, resulting from light diffraction of an object considered as opaque and rough surface in this paper. Interference fringes produced from the coherent mixing are recorded by an image sensor (CMOS or CCD). The Figure 1 illustrates the basic principle. Under the condition that the hologram is correctly recorded [1] (Shannon conditions in particular), we can get an image of the object wavefront from digital reconstruction of the hologram. The complex field of the object is obtained by Single Fast Fourier Transform (S-FFT) algorithms or Double Fast Fourier Transform (D-FFT) with or without variable

magnification [2]. The result of the numerical calculation of the diffracted field gives access to a complex amplitude $O_0(x, y)$ sampled on a grid corresponding to the number of reconstruction points of the algorithm. The Figure 2 illustrates the principle of digital reconstruction leading to possible focus on 2 images (Hermitian symmetry property of the Fourier transform). From the complex amplitude, one can access to the following quantities: the amplitude image (modulus) and phase image (argument of the field). We denote A_r the reconstructed field of the modulus and ψ_r its phase, namely:

$$A_r(x, y) = |O_0(x, y)|, \quad (1)$$

$$\psi_r(x, y) = \arctan\left\{\frac{\Im m[O_0(x, y)]}{\Re e[O_0(x, y)]}\right\} \bmod(2\pi). \quad (2)$$

The phase of the field is calculated by an arctangent function, and consequently result is restricted on the interval $[-\pi, +\pi]$, modulo 2π . Phase is randomly distributed for most cases because it is linked to the roughness of the surface object. The reconstructed object is then degraded by speckle noise. Phase estimation of the reconstructed optical field is the key to a large number of digital holography applications. Particularly, we are interested in studying acoustic phenomena using a technique of ultra-fast digital holography (acquisition of holograms up to 100kHz). Notice that the reconstructed amplitude is amplitude modulated by a speckle pattern due to the coherent light. This speckle is therefore a multiplicative noise. For metrology applications, only optical phase is of interest. Then, one focuses on phase changes over time. The amount assessed is a phase difference between two instants, allowing to follow the evolution of a phenomenon over time. Due to Doppler effect, the phase difference is proportional to the displacement field of the object between the two instants. The optical phase being computed by an arctangent function, equation (2), so it is wrapped. To access physical kinematic quantities on the object, phase must be unwrapped.

**Fig. 1.** Holography principle.**Fig. 2.** Illustration of digital reconstruction.

1.2. Speckle noise on the phase

Commonly, when the object is distorted under any solicitation, which may be mechanical, acoustic, thermal, etc ... it appears a phenomenon of speckle decorrelation [3]. This decorrelation adds a high spatial frequency noise to useful signal. Its spatial correlation width is related to the size of observable speckle grain on the amplitude image. Thus, the phase map requires a filtering process stage in order to be correctly exploited for a confrontation with a physical model of the studied object. The speckle decorrelation has been studied by some authors [4–7]. Phase decorrelation is described statistically by second order properties. Decorrelation can be highlighted from differences of two phases measured at two different instants. Raw hologram phase is random and has speckle properties because it is directly related to the roughness surface of the object illuminated by the laser. Correlation properties on phase or on phase differences are related to the second order probability density function of phase [8]. The calculation of joint probability density function of two speckle phases ψ_1 and ψ_2 has been described in [9, 10]. Given ε the noise induced by speckle decorrelation between two extracted phases at two different moments and $\Delta\varphi$ the phases variation due to structure vibration, then it comes $\psi_2 = \psi_1 + \varepsilon + \Delta\varphi$. $\Delta\varphi$ is considered as a deterministic variable. The probability density function of ε depends on the modulus of complex coherence factor between two speckle fields noticed μ . With variable $\beta = |\mu| \cos(\varepsilon)$, the probability density function on

phase noise ε is given by:

$$p(\beta) = \frac{1 - |\mu|}{2\pi} (1 - \beta^2)^{-3/2} \left(\beta \arcsin \beta + \frac{\pi\beta}{2} + \sqrt{(1 - \beta^2)} \right). \quad (3)$$

The equation (3) describes the probability of noise ε on the difference between two instants. Note that in [4] M. Lehmann discussed the case of speckle spatially resolved and unresolved whereas it is the case of a smooth reference wave (digital holography) or itself speckle (interferometry). In [4], the probability density function of decorrelation induced on the phase is calculated by taking into account the total number of speckle by pixel, which depends on the ratio between the movement of the speckle sensor plane and the pixel size sensor. Note also that ultra-fast holographic method rather concerns case of well resolved speckle, i.e. several pixels by speckle grain, from 3 to 4. Although equation (3) is calculated without regard to the pixel active surface (speckle resolved or not), it depends only on the modulus of correlation factor $|\mu|$. Curves from equation (3) and those of equations given in [4] are similar. We can deduce that equation (3) may be used as a relevant feature to compare decorrelation effect in the different studied cases, correlation factor $|\mu|$ being a marker for quality of extracted data from holograms. For example, the high-speed recording of holograms with low dynamics induces fluctuations in the recording, which are reflected in phase measurements with the same influence as the physical speckle decorrelation due to possible deformation surface. Various methods have been applied to smooth these digital fringes but they have had partial success [11]. Although low-pass filtering is effective in reducing speckle noise [12], it does not preserve the details of phase changes. In this article, we present a comparison between various processing algorithms that we applied to the case of noisy phase. Generally, to preserve 2π phase jumps in the wrapped phase map, the filter is applied on sine and cosine of the phase variations. The type of image noise to deal depends on how to proceed.

2. SPECKLE REDUCING METHODS

2.1. Spatial filtering

The median filter is a basic algorithm which is known to be very efficient to denoise images corrupted by impulse noise. The median filter is easy to implement and generally constitutes a reference method to evaluate other more complex algorithms.

2.2. Wiener filter

The Wiener filter is the solution of the minimization of the mean square error computed between the original image s and the filtered image, in case of linear blurring model with additive noise ε . Reminder [13] the transfer function $W(u, v)$ is

given by:

$$W(u, v) = \frac{H(u, v)^* \Phi_s(u, v)}{|H(u, v)|^2 \Phi_s(u, v) + \Phi_b(u, v)}. \quad (4)$$

In equation (4) the spreading function $H(u, v)$ is chosen to be neutral, i.e. unitary. The power spectrum densities of original image and noise are not known a priori, and they are replaced by estimators based on median filtering of noisy image in place of the original image, and difference of the two last images for noise.

2.3. SAR filtering

The SAR (Synthetic Aperture Radar) images exhibits the same properties as that of speckle images. Especially, the noise model is considered as multiplicative. The Lee filter [14] is an adaptive filter in which the parameters are adapted according to local statistical properties of the image to be processed. These parameters are estimated in a window centered on the pixel for which one we expect restoring the correct value:

$$d(i, j) = \alpha \cdot s(i, j) + (1 - \alpha) \cdot \overline{s(i, j)}. \quad (5)$$

In equation (5), $d(i, j)$ is the enhanced image, $s(i, j)$ is the noisy image ($\bar{s}(i, j)$ the mean value) and α depends on the ratio of the squares of local variations of the image and noise, $\alpha = 1 - C_n^2/C_s^2$. The local variation coefficient is defined as the ratio of variance by mean square of the pixel values. If the variation in the observed image is less than that of the noise, α is equal to 0, and the average of the window is affected to the pixel value. In the opposite case, if this variation is greater than that of the noise, the current value of the pixel is saved. Frost filter [11] is an adaptive Gaussian filter kernel. Kernel parameters are adjusted according to the local statistics of the image under square shape of the local variation coefficient C_s^2 . In a region of homogeneous values the local coefficient variation is low, the filter behaves as an averaging. In the presence of an edge or a discontinuity, the coefficient increases and the Gaussian kernel is concentrated around current pixel, ultimately its original value is retained.

2.4. Wavelets thresholding approaches

The denoising method using a decomposition on a wavelet basis associated with a threshold function has already been discussed in the field of image enhancement [15, 16]. Its principle consists in applying a threshold operator on wavelet coefficients computed from the image to be processed. When the wavelet basis is adapted to signal contents, its representation in the wavelet coefficients space is sparse, meaning that all the information is concentrated in the highest coefficients. The idea is then to apply a threshold and consequently leaves off least significant coefficients which are supposed to mainly

contain noise. In this approach, noise is supposed to be additive. Considering wavelet transform, the same model applies on the coefficients. In the case of multiplicative noise, a transformation applies a logarithm before the threshold leads to an equivalent model, this principle has been studied in the case of speckle noise processing in SAR images [17]. Multiple variants of solutions that we will not detail here are available from the multiple parameters of this method: choice of the wavelet base, number of decomposition levels, profile of the thresholding operator, threshold values and their different associated estimator. This work was focused, on one hand, on separable wavelets Daubechies and symlets builds from the tensor product of their 1D release, and, on the other hand, on curvelets [18] builds in a circular paving plan and offers a wide range of orientation waveforms.

2.5. Non-local means method

Non local means method (NL-means), recently proposed [19, 20], is an efficient technique for the enhancement of images corrupted by noise. Its principle is based on pixels value replacement by a weighted sum of values included in patches that are chosen in the neighbourhood of the pixel to be processed. The weighting is obtained from correlations estimated between the local patch of the pixel to be processed and the patch of the neighbourhood patches that are taken into account in the algorithm. Thus, when a patch is strongly correlated with the local patch of the pixel to be processed, the pixel is taken into account in the weighting with a coefficient evaluated from a gaussian kernel which argument is the euclidean distance between the two patches. Such method was already used with success for speckle images from digital holography but with a different methodology approach (blind criterion without a reference image) [21].

3. EVALUATION CRITERIA

The test set consists of the simulated interference fringes phase images in which the noise level is controlled. For each test, three evaluation criteria are computed. The first one is the gain of SNR (G_{SNR}),

$$G_{SNR} = R_{SNR} - I_{SNR}. \quad (6)$$

In this expression R_{SNR} and I_{SNR} are respectively SNR measured at the input and the output of the noise processing stage, given in dB unit. The residual SNR R_{SNR} , is defined from original (non noisy) image $s(i, j)$ and denoised image $d(i, j)$ as:

$$R_{SNR} = 10 \log 10 \left(\frac{\sum_{ij} s(i, j)^2}{\sum_{ij} (s(i, j) - d(i, j))^2} \right). \quad (7)$$

Although used to evaluate numerous works on enhancement and image restoration, SNR and its variants have a significant

drawback because it is based on the calculation of an averaged error which does not account for distortions affecting structures of an image. Thus the same amount of error can be observed between two images restored for a perceived image quality very different. To this end, the "Quality index" criterion, Q_{index} , proposed by Wang and Bovik [22] better reflects the quality perceived image. Its calculation is based on the product of three components:

$$Q_{index} = \frac{\sigma_{sd}}{\sigma_s \sigma_d} \cdot \frac{2\mu_s \mu_d}{\mu_s^2 + \mu_d^2} \cdot \frac{2\sigma_s \sigma_d}{\sigma_s^2 + \sigma_d^2} \quad (8)$$

In this expression, μ_s and μ_d represent the mean of pictures s and d , respectively the original image and the processed image; σ_s and σ_d are their variances and σ_{sd} their covariance. One can notice that Q is bounded by values -1 and $+1$, the latter is reached when two images are identical in every way. This criterion was also selected by the authors of a recent publication [11] dealing with noising interferograms. Since the ultimate goal involves reconstruction of interferogram phase map, the third criterion is based on the error on phase reconstruction. It is calculated from images with pure and denoised phases reconstructed from images processed with sine and cosine. The phase error is then obtained from the computation of the empiric standard deviation σ_ϕ of pixels amplitude distribution.

4. RESULTS AND DISCUSSION

Simulation results are reported in Table 1. on three columns: G_{SNR} , σ_ϕ and Q_{INDEX} . We can clearly see that methods based on wavelet transforms exhibits best results in terms of phase error. So, for low SNR until 10 dB, curvelets performs the best, from medium SNR, Daubechies wavelets and for high SNR (from 12.5 dB) symlets are the best. In order to have a qualitative point of view of how curvelets processing works, a simulation exemple is reported in Figure 3. Very good results are obtained with Wiener filter for phase error, which is also better than that curvelets for input SNR equal to 10 dB.

In terms of SNR gain, best results are obtained with symlets except for the median filter at 5 dB. The NL-means method exhibits results that are quite equivalent to those given by SAR methods. However, the NL-means method is particularly not suited to the phase restoration since it globally exhibits bad results both in terms of phase error and SNR gain. Until 10 dB the two SAR methods give worst results than those given by simple median filter in term of phase error and SNR gain, and this in spite of conditions of realization of noise that are close to the two applications (SAR and digital holography).

In terms of quality index Wiener filter performs very well and is the most efficient among all other methods. From 12.5 dB, all methods gives results very closed each other and below,

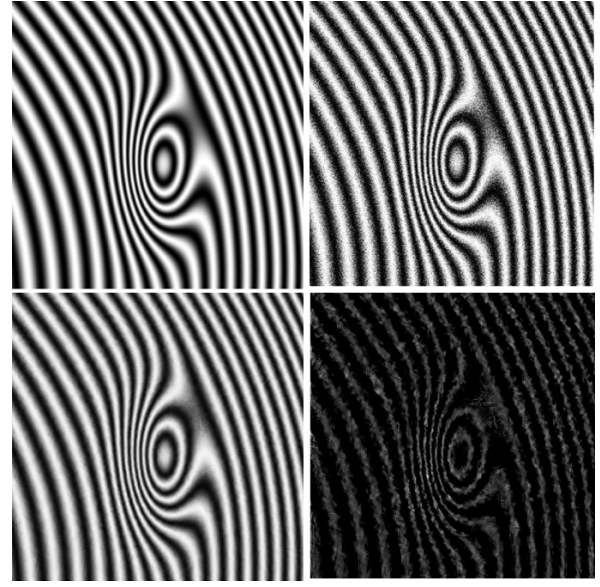


Fig. 3. Phase denoising with curvelets method. Input SNR is equal to 7.5 dB. From left to right and top to bottom: cosine image of respectively pure phase, noisy phase, denoised phase and removed noise.

except Wiener filter and curvelets, all methods degrades significantly.

5. CONCLUSION

This paper presents a comparison of image denoising algorithms applied to the processing of phase data images degraded with speckle noise in the context of digital holography. Evaluations are achieved on simulated interference fringes images degraded with controlled noise level. As main results, curvelets and symlets demonstrated most efficiency, in terms both of gain of SNR and of phase error. These approaches surpasses algorithms used for SAR images processing, which, however, use the same noise model as inherent to the phase fringe patterns. We expect addressing the reconstruction problem of locally dislocation in phase maps, in a near future. To do this, we will consider curvelets associated with sparse constraints.

This research is funded from the French National Agency for Research (ANR) under grant agreement number ANR-14-ASTR-0005-02.

REFERENCES

- [1] P. Picart and J. Leval, "General theoretical formulation of image formation in digital fresnel holography," *J. Opt. Soc. Am. A*, vol. 25, 2008.

- [2] P. Picart and J.C. Li, *Digital holography*, ISTE-Wiley, London, 2012.
- [3] P. Owner-Petersen, “Decorrelation and fringe visibility: on the limiting behavior of various electronic speckle-pattern correlation interferometers,” *J. Opt. Soc. Am.A*, vol. 8, 2008.
- [4] M. Lehmann, “Decorrelation-induced phase errors in phase shifting speckle interferometry,” *Appl. Opt.*, vol. 36, 1997.
- [5] M. Lehmann, “Phase-shifting speckle interferometry with unresolved speckles: A theoretical investigation,” *Opt. Comm.*, vol. 128, 1996.
- [6] M. Lehmann, “Optimization of wave-field intensities in phase-shifting speckle interferometry,” *Opt. Comm.*, vol. 118, 1995.
- [7] P. Picart, J. Leval, D. Mounier, and S. Gougeon, “Time-averaged digital holography,” *Optics Letters.*, vol. 28, 2003.
- [8] J. C. Dainty, A. E. Ennos, M. Franon, J.W. Goodman, T. S. McKechnie, and G. Parry, *Laser Speckle and Related Phenomena*, ISTE-Wiley, Berlin, 1975.
- [9] D. Middleton, *Introduction to Statistical Communication Theory*, Mc Graw Hill, New York, 1960.
- [10] W. B. Davenport and W. L. Root, *Random Signals and Noise*, Mc Graw Hill, New York, 1958.
- [11] A. Frederico and G. H. Kaufmann, “Denoising in digital speckle pattern interferometry using wave atoms,” *Optics Letters*, vol. 32, no. 10, pp. 1232–1234, 2007.
- [12] H.A. Aebsicher and S. Waldner, “A simple and effective method for filtering speckle-interferometric phase fringe patterns,” *Optics Communications*, vol. 162, no. 4-6, pp. 205–210, 1999.
- [13] R. C. Gonzales and R. E. Woods, *Digital image processing*, Addison-Wesley Company.
- [14] Lee J.S., “Digital image enhancement and noise filtering by using local statistics,” *IEEE Trans. Pattern Anal. Machine Intelligence*, 1980.
- [15] S. G. Mallat, *A wavelet tour of signal processing*, Academic Press, San Diego, 1999.
- [16] D. L. Donoho, “De-noising by soft-thresholding,” *IEEE Transactions on Information Theory*, vol. 41, no. 3, pp. 613–627, May 1995.
- [17] H. Xie, L. E. Pierce, and F.T. Ulaby, “Sar speckle reduction using wavelet denoising and markov random field modeling,” *IEEE Trans. Geosci. Remote Sens.*, vol. 40, no. 10, pp. 2196–2212, 2002.
- [18] J.L. Starck, E. J. Candes, and D. L. Donoho, “The curvelet transform for image denoising,” *IEEE Trans. Image Process.*, vol. 11, no. 6, pp. 670–684, June 2002.

Table 1. Results

$I_{SNR}(dB)$	Method	$G_{SNR}(dB)$	σ_ϕ (rad.)	Q_{index}
5.0	Frost	7.8	0.2745	0.4
	Frost	8.4	0.1937	0.5
	Frost	8.6	0.1369	0.7
	Frost	8.1	0.1014	0.8
	Frost	7.2	0.0738	0.8
7.5	Lee	7.1	0.1965	0.4
	Lee	7.6	0.1454	0.5
	Lee	8.1	0.1062	0.7
	Lee	8.1	0.0804	0.8
	Lee	8.1	0.0589	0.9
10.0	Median	9.7	0.1645	0.3
	Median	9.5	0.1263	0.5
	Median	9.0	0.0996	0.6
	Median	8.0	0.0831	0.7
	Median	6.8	0.0695	0.8
12.5	NL-means	7.9	0.1989	0.3
	NL-means	8.4	0.1346	0.5
	NL-means	8.3	0.0948	0.7
	NL-means	7.6	0.0725	0.8
	NL-means	6.4	0.0580	0.9
15.0	Wiener	8.8	0.1077	0.8
	Wiener	9.8	0.0794	0.7
	Wiener	10.2	0.0619	0.8
	Wiener	9.6	0.0503	0.8
	Wiener	8.3	0.0431	0.9
5.0	Curvelets	8.7	0.0903	0.6
	Curvelets	9.7	0.0756	0.6
	Curvelets	10.6	0.0622	0.7
	Curvelets	10.7	0.0511	0.7
	Curvelets	10.8	0.0406	0.8
7.5	Daub 4	9.5	0.0974	0.3
	Daub 4	10.5	0.0762	0.5
	Daub 4	11.2	0.0591	0.6
	Daub 4	11.2	0.0461	0.7
	Daub 4	11.0	0.0359	0.8
10.0	symlets 6	9.5	0.0992	0.3
	symlets 6	10.6	0.0772	0.4
	symlets 6	11.3	0.0596	0.6
	symlets 6	11.4	0.0461	0.7
	symlets 6	11.5	0.0351	0.8
12.5				
15.0				
19.0				
20.0				
21.0				
22.0				